Acta Oceanol. Sin., 2019, Vol. 38, No. 12, P. 26–34
https://doi.org/10.1007/s13131-019-1513-4
http://www.hyxb.org.cn
E-mail: hyxbe@263.net

N_2 fixation rate and diazotroph community structure in the western tropical North Pacific Ocean

Run Zhang[1]*, Dongsheng Zhang[2], Min Chen[1], Zhibing Jiang[2], Chunsheng Wang[2]*, Minfang Zheng[1], Yusheng Qiu[1], Jie Huang[3]

[1] College of Ocean and Earth Sciences, Xiamen University, Xiamen 361102, China

[2] Key Laboratory of Marine Ecosystem and Biogeochemistry, State Oceanic Administration/Second Institute of Oceanography, Ministry of Natural Resources, Hangzhou 310012, China

[3] Ministry of Education Key Laboratory for Earth System Modeling/Department of Earth System Science, Tsinghua University, Beijing 100084, China

Received 28 December 2018; accepted 19 February 2019

Abstract

In the present study, we report N_2 fixation rate (^{15}N isotope tracer assay) and the diazotroph community structure (using the molecular method) in the western tropical North Pacific Ocean (WTNP) (13°–20°N, 120°–160°E). Our independent evidence on the basis of both *in situ* N_2 fixation activity and diazotroph community structure showed the dominance of unicellular N_2 fixation over majority of the WTNP surface waters during the sampling periods. Moreover, a shift in the diazotrophic composition from unicellular cyanobacteria group B-dominated to *Trichodesmium* spp.-dominated toward the western boundary current (Kuroshio) was also observed in 2013. We hypothesize that nutrient availability may have played a major role in regulating the biogeography of N_2 fixation. In surface waters, volumetric N_2 fixation rate (calculated by nitrogen) ranged between 0.6 and 2.6 nmol/(L·d) and averaged (1.2±0.5) nmol/(L·d), with <10 μm size fraction contributed predominantly (88%±6%) to the total rate between 135°E and 160°E. Depth-integrated N_2 fixation rate over the upper 200 m ranged between 150 μmol/(m^2·d) and 480 μmol/(m^2·d) (average (225±105) μmol/(m^2·d). N_2 fixation can account for 6.2%±3.7% of the depth-integrated primary production, suggesting that N_2 fixation is a significant N source sustaining new and export production in the WTNP. The role of N_2 fixation in biogeochemical cycling in this climate change-vulnerable region calls for further investigations.

Key words: western tropical North Pacific Ocean (WTNP), N_2 fixation, ^{15}N isotope tracer assay, unicellular diazotroph

Citation: Zhang Run, Zhang Dongsheng, Chen Min, Jiang Zhibing, Wang Chunsheng, Zheng Minfang, Qiu Yusheng, Huang Jie. 2019. N_2 fixation rate and diazotroph community structure in the western tropical North Pacific Ocean. Acta Oceanologica Sinica, 38(12): 26–34, doi: 10.1007/s13131-019-1513-4

1 Introduction

N_2 fixation plays a major role in adding biologically essential N nutrients and drive biogeochemical cycles for the oligotrophic tropical/subtropical oceans (Gruber and Sarmiento, 1997; Karl et al., 2002; Deutsch et al., 2007). The western tropical North Pacific Ocean (WTNP) is a region of significant importance to global climate system and fisheries wherein material and heat exchanges take place actively (Lehodey et al., 1997; Carpenter, 1998; Clement and DiNezio, 2014). The WTNP also seems as a favorable environment for N_2 fixation as it is characterized by low nutrient low chlorophyll (LNLC) conditions in the permanently stratified upper water column (Cabrera et al., 2015). However, our knowledge of N_2 fixation is not abundant in the WTNP in general.

Available N_2 fixation data are few and directly measured rates are far from abundant in the WTNP (Kitajima et al., 2009; Shiozaki et al., 2013; Chen et al., 2014; Kim et al., 2017). At a fixed station (13°N, 135°E) in the Western Pacific Warm Pool, $^{15}N_2$ tracer assay based N_2 fixation rate fell in a range of 1–15 μmol/(m^3·d) for the upper water column, likely suggesting that the Western Pacific Warm Pool, and probably the adjacent waters also, is suitable for N_2 fixation (Shiozaki et al., 2013). In general, large spatial scale sampling spanning the WTNP is lacking to date. Besides the N_2 fixation rate, the diazotroph community structure is a key variable factor when looking into the dynamics of N_2 fixation and evaluating its biogeochemical importance in the context of the ongoing rapid climatic changes (Church et al., 2009; Fu et al., 2014). The filamentous cyanobacterium *Trichodesmium* (Capone et al., 1997) and heterocystous endosymbiont *Richelia* (Carpenter et al., 1999) had traditionally been considered as the dominant oceanic N_2 fixers. Recently, using molecular approaches targeting the *nifH* gene, marine diazotrophs including unicellular cyanobacteria (groups UCYN-A, -B, -C) and non-cyanobacterial diazotrophs (bacteria and archaea) are widely distributed and actively fix N_2 in global oceans (Zehr et al., 2001; Church et

Foundation item: The National Basic Research Program of China under contract No. 2015CB452903; the Foundation of China Ocean Mineral Resources R&D Association under contract No. DY135-E2-2-03; the Science and Technology Basic Resources Investigation Program of China under contract No. 2017FY201403; the National Natural Science Foundation of China under contract Nos 41676174, 41206104 and 41876198.

*Corresponding authors, E-mail: zhangrun@xmu.edu.cn; wangsio@sio.org.cn

al., 2008; Shiozaki et al., 2014). Studies have also indicated that the UCYN-A (*Atelocyanobacterium*) and UCYN-B (*Crocosphaera*) may equally contribute to or even exceed the amount of N_2 fixed by *Trichodesmium* in some regions in the oligotrophic Pacific Ocean (Zehr et al., 2001; Montoya et al., 2004). Diazotroph community structure and activity along a long south-north transect between the central equatorial Pacific and the Bering Sea had been examined, revealing large latitudinal variability in the western Pacific (Shiozaki et al., 2017). However, the composition and zonal pattern of diazotrophic groups and their relative contribution to N_2 fixation contribution in the WTNP remain largely unknown.

In the present study, large spatial range sampling in the WTNP were conducted to (1) measure the N_2 fixation rate; (2) examine the bulk N_2 fixation rate and of two size fractions (10 μm as a category); and (3) diazotroph community structure, which is vital to understanding N_2 fixation dynamics and its biogeochemical impact in the WTNP. Our results will add knowledge concerning N_2 fixation in the undersampled WTNP and provide insights to understand C and N dynamics in the WTNP, which is now experiencing significant environmental changes (Cravatte et al., 2009).

2 Materials and methods

2.1 *Oceanographic setting*

The westward-flowing North Equatorial Current (NEC) is a prevailing surface current in the sampling area (13°–20°N) of the WTNP, and plays a vital role in the North Pacific circulation as it partitions the flow to the subtropical gyre to the north and the tropical gyre to the south (Qiu et al., 2015). The NEC bifurcates at ~13°N when meeting the western boundary and flows northward as the Kuroshio and southward as the Mindanao Current (Qiu et al., 2015) (Fig. 1). Outside the sampling area, surface currents also include the eastward North Equatorial Countercurrent (NECC) in the south and the eastward North Pacific Subtropical Countercurrent (STCC) in the north. The WTNP is featured by strong light radiation. Due to surface stratification over almost the entire year, the WTNP is oligotrophic with low levels of nutrients and chlorophyll *a* (Cabrera et al., 2015).

2.2 *Seawater sampling*

A total of 38 stations were sampled on cruises DY27-1 (8–26 July 2012), DY27-2 (20–22 August 2012), DY27-3 (8–19 September 2012), and west–east DY29-1 (30 May–4 June 2013) onboard the R/V *Haiyang Liuhao* in the WTNP, covering a spatial range ~14°–20°N, 120°–160°E (Fig. 1). Seawater samples were collected from 0, 30, 50, 75, 100, 150, 200 m using a Niskin bottle rosette sampler attached with conductivity-temperature-depth (CTD) sensors (SBE 917Plus, Sea-Bird) or an acid-cleaned bucket. Ocean Data View was used to draw sampling maps.

2.3 *Environmental variables*

The chlorophyll *a* concentration was determined using a Turner Trilogy fluorometer while on the sea. Macro-nutrients were measured after conventional protocols (Hansen and Koroleff, 1999). Nitrate and nitrite were measured on a SKALAR SAN++ flow injection autoanalyzer after reduction using the cadmium–copper reduction method. The detection limit for nitrate analysis was 0.2 μmol/L in the range of 0.2–10 μmol/L. Phosphate was determined by the standard molybdenum blue method with a detection limit of 0.02 μmol/L.

2.4 *Nitrogen isotopic ratio of suspended particulate organic matter ($\delta^{15}N_{PN}$)*

Bulk suspended particulate organic nitrogen (PN) for meas-

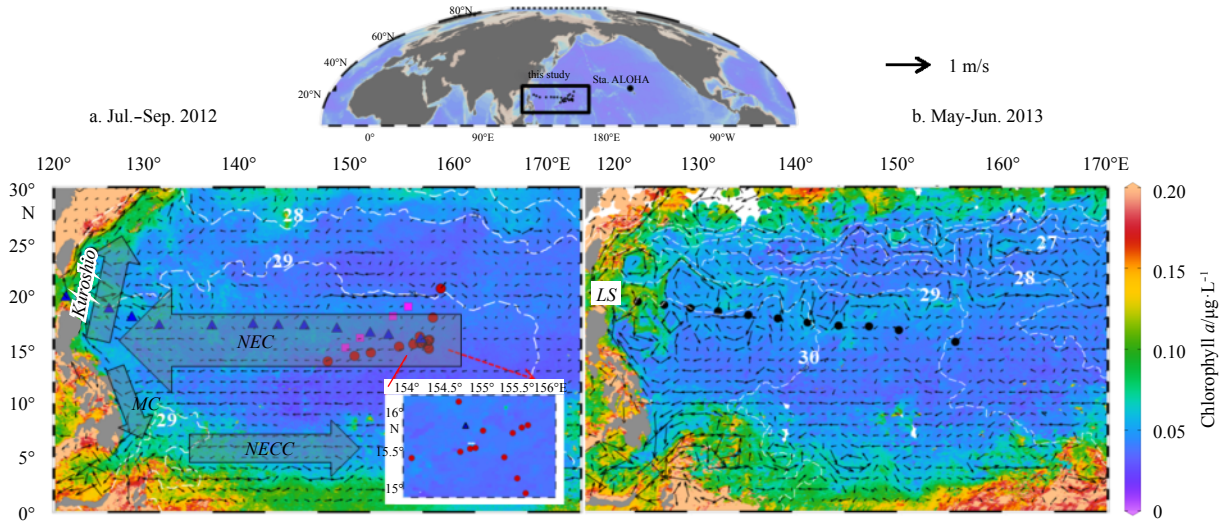

Fig. 1. Sampling locations in the WTNP during 2012 (a) and 2013 (b) cruises. Background contours, vectors, and white dashed isolines represent satellite-derived mean chlorophyll *a*, geostrophic current, and SST (°C) during the study periods (July–September 2012 and May–June 2013). The inset map on the left panel indicates sampling locations around the Magellan Seamounts. Red dots: 8–26 July 2012; violet squares: 20–22 August 2012; blue triangles: 8–19 September 2012; black dots: 30 May–3 June 2013. LS represents Luzon Strait, MC Mindanao Current, NEC North Equatorial Current, and NECC North Equatorial Counter Current. Satellite data sources: 4 km monthly chlorophyll *a* data from Aqua Moderate Resolution Imaging Spectroradiometer (MODIS, https://oceandata.sci.gsfc.nasa.gov/MODIS-Aqua/Mapped/); (1/4)° daily Advanced Very-High-Resolution Radiometer (AVHRR) SST data provided by NOAA (National Oceanic and Atmospheric Administration, https://www.ncdc.noaa.gov/oisst/data-access); (1/4)° daily surface geostrophic current released by Archiving, Validation and Interpretation of Satellite Oceanographic data (AVISO, https:/www.aviso.altimetry.fr/en/data.html).

uring natural ^{15}N abundance was collected from 0, 30, 50, 75, 100, 150, 200 m by filtering ~10 L of seawater onto precombusted (450°C, 4 h) GF/F glass fiber filters. The filters containing POM were stored frozen (–20°C) while on the sea. PN content and ^{15}N abundance were measured on a Finnigan MAT DELTA^{plus} XP isotope ratio mass spectrometer that was coupled to a Carlo Erba NC2500 elemental analyzer (EA-IRMS). Nitrogen isotopic composition was presented in the conventional δ notation as follows:

$$\delta^{15}\mathrm{N} = \left(\frac{R_{\mathrm{sample}}}{R_{\mathrm{standard}}} - 1\right) \times 1\,000, \quad (1)$$

where R_{sample} and R_{standard} are the $^{15}N/^{14}N$ ratios of the sample and the standard air N_2, respectively. International isotope reference materials (IAEA-N-2 and USGS35) were used for calibration. The reproducibility of $\delta^{15}N$ measurements was better than 0.2‰. To measure size fractionated $\delta^{15}N_{PN}$, ~25 L of surface seawater was prefiltered through a Millipore polycarbonate (pore size 10 μm) membrane and then by a GF/F membrane at seven stations. The particles collected on the GF/F filter are of the <10 μm size class. Particles collected on the prefilter were washed onto a GF/F filter and are thus of the >10 μm size class. The filter samples were frozen while on the sea. The validation of the size fractionation experiment was conducted at seven stations (see Supplementary Information).

2.5 *N_2 fixation rate (NFR)*

Vertical samples for incubation of N_2 fixation and primary production were collected at nine stations down to 200 m during the 2012 cruise. N_2 fixation rates were measured using $^{15}N_2$ tracer assay (Montoya et al., 1996). The technique is the same as Zhang et al. (2015). Briefly, the duplicate seawater samples in clear transparent glass bottles were amended with $^{15}N_2$ (2 mL $^{15}N_2$ per L seawater) and fitted with screens to simulate light intensities (0 m: 100%; 25 m: 50%; 50 m: 10%; 100 m: 1%; 150 m: 1%; 200 m: 0.1%), and then placed in a deck incubator with flowing surface seawater for 24 h. The depth-integrated rate was obtained after trapezoidal integration. The rate obtained using this method may represent underestimates due to the insufficient dissolution of $^{15}N_2$ gas (Mohr et al., 2010). However, we suggest that this factor did not undermine our discussion, mainly the degree of underestimation of absolute rates will be significantly lowered after 24 h incubation (Klawonn et al., 2015; Wannicke et al., 2018). Second, the size characteristics of NFR will be slightly affected compared to that of the absolute NFR.

Post-incubation NFR size fractionation (Bonnet et al., 2009) was conducted at seven stations. Each incubated sample was prefiltered through a Millipore polycarbonate filter (pore size 10 μm) and then by a precombusted glass fiber filter. The particles collected on the GF/F filter are of the <10 μm size class. The particles collected on the polycarbonate prefilters were transferred to another glass fiber filter and thus are of the >10 μm size class. The size fractionated samples were frozen while on the sea. N_2 fixation samples were also measured on EA-IRMS for PN content and ^{15}N abundance. The contribution of each size fraction to the total NFR was estimated subsequently.

2.6 *Nitrogenase gene (nifH) analysis-derived diazotroph community structure*

During the 2013 cruise, diazotroph community structure at the genus level was examined based on nitrogenase (*nifH*) relative abundance at 11 stations (P1–P11) along a meridional section (125°–155°E). Surface (~0 m) seawater samples were collected at 10 stations (P1–P10), while depth profile down to 100 m (25, 50, 75 and 100 m) was sampled at the easternmost Sta. P11. For each sample, ~4 L of seawater was filtered onto a polycarbonate filter (0.2 μm poresize, Millipore) after being prefiltered through a 200 μm mesh size silk and then frozen immediately in liquid N_2 until extraction in the land laboratory. The filters were cut into small pieces with pre-sterilized scissors and then transferred into tubes. Then, the total DNA was extracted using a Fast DNA Spin kit (MP Biomedicals, USA) based on the manufacturer's protocols.

The nitrogenase gene (*nifH*) was amplified using a nested Polymerase Chain Reaction (PCR) protocol (Zehr and Turner, 2001). The reaction mixture (50 μL final volume) contained 5 μL PCR 10× buffer (TaKaRa, China), 8 μL of a 25 mmol/L $MgCl_2$ solution, 8 μL of 200 mmol/L dNTPs (TaKaRa, China), 0.5 μL of each primer (100 μmol/L, Sangon Biotech, China), 0.5 μL of Taq DNA polymerase (TaKaRa, China), 2 μL template, and 25.5 μL of deionized water. For each DNA extraction sample, triplicate PCR reactions were conducted with one additional negative control. Primers used in the first-round PCR reaction were *nifH*3 (5′-TTYTAYGGNAARGGNGG-3′) and *nifH*4 (5′-ATRTTRTT NGCNGCRTA-3′). In the second-round PCR reaction, *nifH*1 and *nifH*2 were used with adaptors and sample specific barcodes added (see Supplementary Information). PCR products of each sample were run on a 1% agarose gel and amplified *nifH* fragments were excised and purified with a QIAquick Gel extraction kit (Qiagen, USA). None of the 11 negative controls resulted in a visible band when run on a gel. Illumina sequencing was performed using a Miseq PE300 kit (Shanghai Majorbio Bio-Pharm Biotechnology Co. Ltd., Shanghai, China). The purified PCR products with specific barcodes were quantified using a QuantiFluor™-ST (Promega).

Pair-end (PE) reads data (raw data) were obtained from Miseq sequencing. The quality control was conducted using Trimmomatic. Bases in the reads end were filtered if the quality value below 20. After this quality control step, the reads with length below 50 bp were removed. The filtered PE reads merged into one sequence, the minimum overlap length was 10 bp. The different samples were separated according to the adaptors and tags, and in the meanwhile the forward-reverse orientation of sequences was adjusted. The adaptors and tags needed to be totally identity and the maximum mismatched base numbers of primers were 2 bp. In total, 554 564 sequences were obtained from 14 samples (Table S1). The trimmed sequences have been deposited in the National Center for Biotechnology Information (NCBI) Sequence Read Archive under accession number SRP 153943.

The unique tags were extracted from the trimmed sequences. The singletons were removed from the unique tags. Then these unique tags were clustered as representative sequences of OTUs by Usearch 7.1 with cutoff value 0.97. The chimera was removed during the clustering process. All unique tags were mapped to the representative sequences of OUTs. The representative sequences of OTUs were assigned to the taxonomy classification by RDP classifier (Wang et al., 2007) within Qiime platform (Caporaso et al., 2010) with FGR database (Fish et al., 2013). The threshold was set as 0.7. According to the taxa classification information, all sequences were regrouped into several *nifH* clusters as follows, those belonging to Cyanobacteria were split into *Trichodesmium*, UCYN-B (*Crocosphaera*) and other cyanobacteria, the other sequences were stayed in class level including Alpha-proteobacterial, Beta-proteobacteria, Delta-proteobacteria, Gamma-proteobacterial, Proteobacteria unclassified, Clostridia and others. The regrouped sequences were used to analyze the community composition of each sample.

2.7 *Primary production*

In the 2012 cruises, primary production (PP) was measured via a ^{14}C tracer assay (Wolfe and Schelske, 1967). Surface (~0 m) samples were collected at 19 stations and depth profiles were collected at three stations (135°, 150°, 155°E). Briefly, 100 mL of seawater was filled into three acid-cleaned transparent polycarbonate bottles (one dark+two light) immediately after collection, and 0.8 μCi $NaH^{14}CO_3$ was then added to each bottle. The bottles were placed in a deck incubator with flowing surface seawater for 24 h. At the end of incubation, each sample was gently (<100 mm Hg) filtered using 0.2 μm-pore size mixed cellulose ester membranes and stored frozen (20°C) while on board. Before analysis, the sample filters were acid fumigated to remove inorganic carbon. The incorporated ^{14}C radioactivity was then measured on a liquid scintillation counter (Perkin-Elmer TriCarb 2900TR). The PP rates (μmol/(L·d), calculate by carbon) were calculated as follows:

$$PP = \frac{(R_S - R_B) \times c_{TCO_2}}{R \times \Delta t}, \quad (2)$$

where R_S and R_B are the radioactivities of ^{14}C (μCi) in light and dark bottles after correction for quenching, respectively. R and c_{TCO_2} are the added radioactivity of $NaH^{14}CO_3$ and the total carbon dioxide (μmol/L, calculated by carbon) in seawater, respectively. To estimate the depth-integrated PP (mmol/(m²·d)), trapezoidal integration was used.

3 Results

3.1 *Environmental variables*

LNLC conditions were observed during sampling (Figs 1 and 2a). Sea surface temperature (SST) generally exceeded 28°C. Not surprisingly, dissolved inorganic nitrogen (nitrate+nitrite) was generally low in the upper water column (100 m) (Fig. 3f). Moreover, low concentrations of soluble reactive phosphorus were observed (Fig. 3g). The shipboard-measured chlorophyll *a* concentration was generally <0.05 mg/m³ in surface waters. Along the meridional section (PO section, ~125°–150°E) sampled in September 2012, relatively higher surface chlorophyll *a* was observed for the western stations located in the Philippine Sea. The depth wherein subsurface chlorophyll maximum (SCM) was present was found to be 75–125 m along the PO section, with an increasing trend westward (Fig. 3e).

3.2 *Natural $\delta^{15}N_{PN}$*

Nitrogen isotopic ratios ($\delta^{15}N$) in natural suspended particulate nitrogen (PN) varied from −1.6‰ to +4.2‰ ((1.9±1.3)‰,

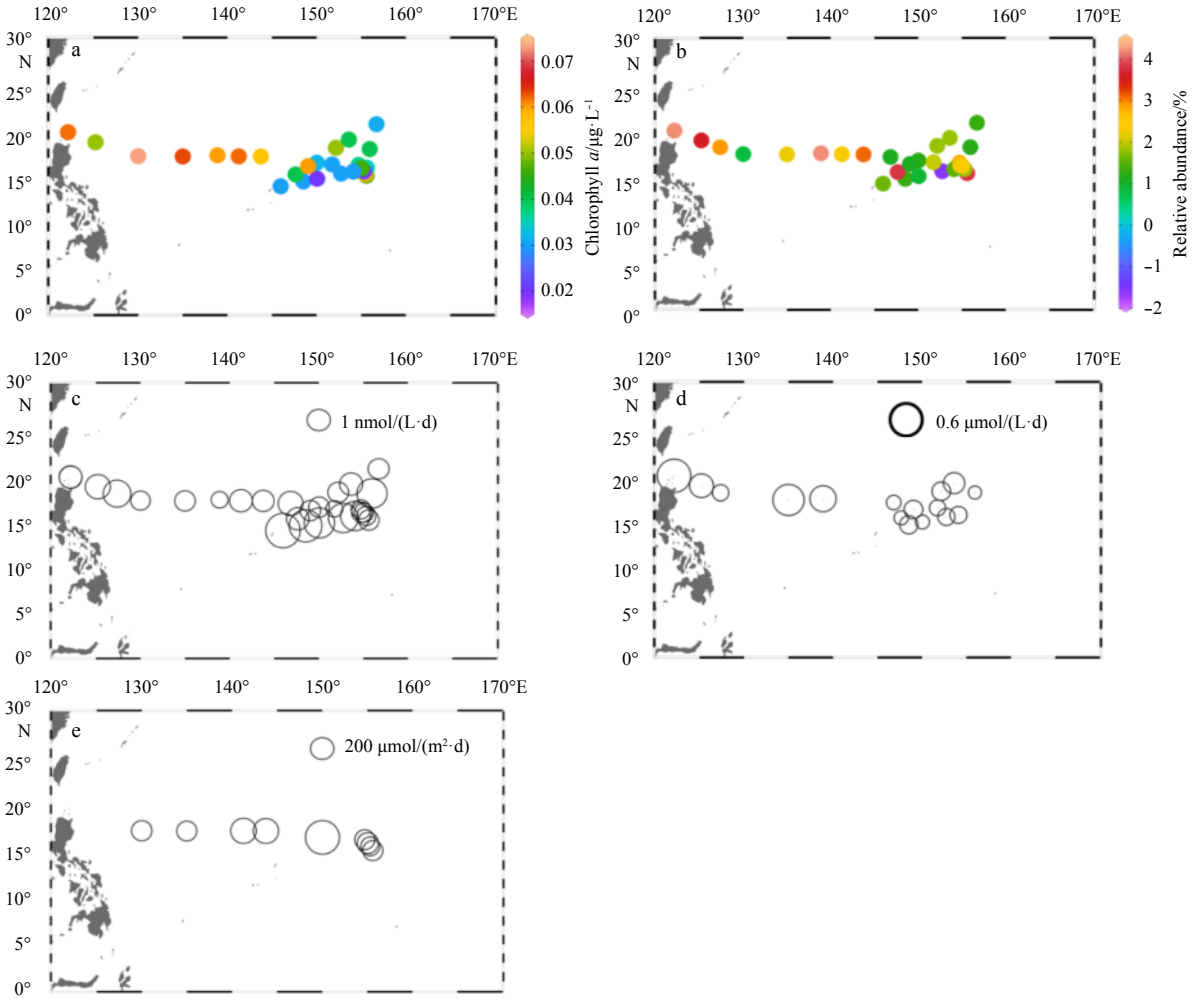

Fig. 2. Surface distributions of chlorophyll *a* concentration (a); suspended $\delta^{15}N_{PN}$ (b); total N_2 fixation rate (c); PP (d); and distribution of depth-integrated N_2 fixation rate (e).

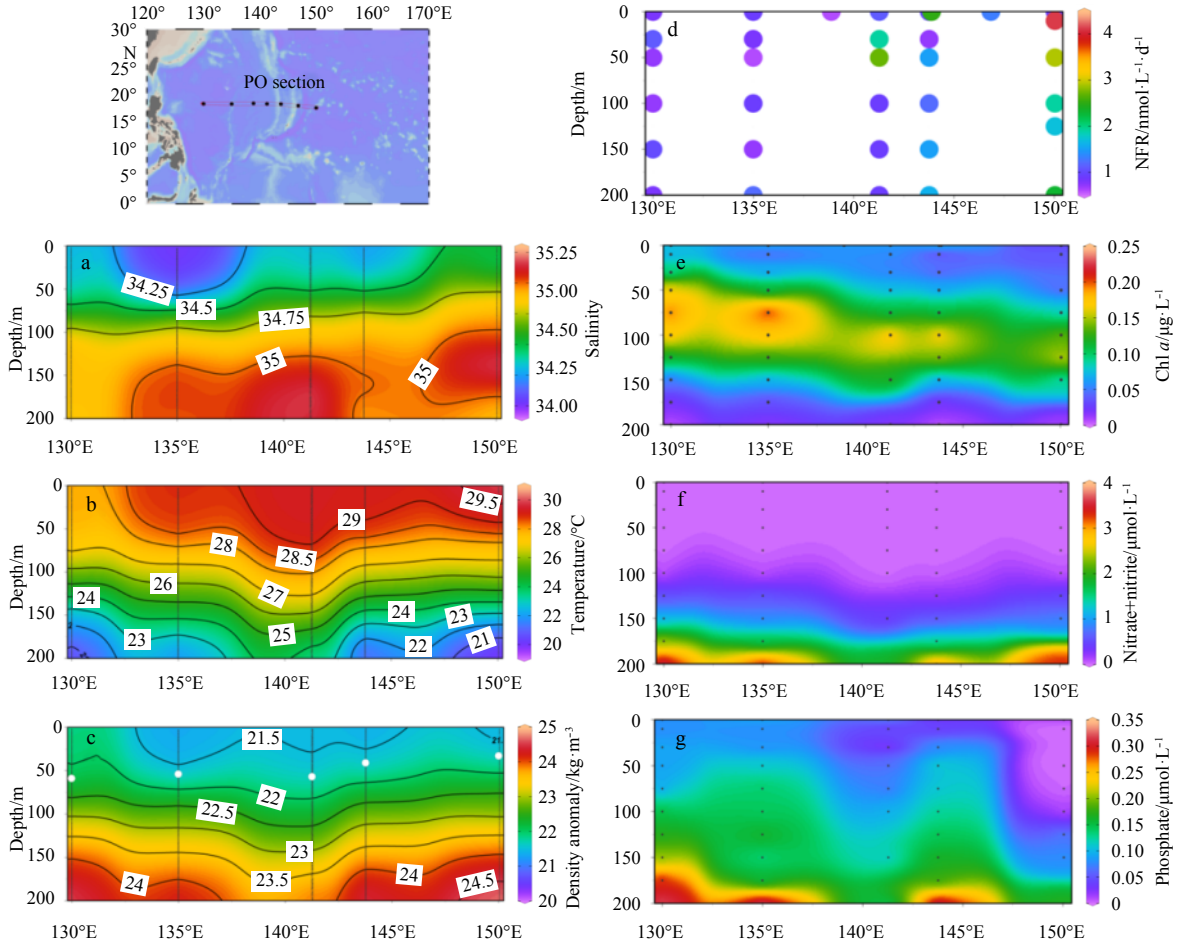

Fig. 3. Depth profiles in the upper 200 m along 17°N during September 2012: salinity (a) and temperature (b) at 1 m interval; density anomaly (c); NFR (d); chlorophyll *a* (e); nitrate+nitrite (f); and phosphate (g). Mixed layer depth (MLD, defined as the depth where the potential density has decreased by 0.125 kg/m^3 relative to 10 m) is indicated by the white dots on the density plot.

n=27) in surface waters (Fig. 2b). Size fractionation experiment of surface suspended particulate organic matter (POM) showed that δ^{15}N in <10 μm PN was significantly lower than that of >10 μm PN ((1.7±1.3)‰ vs (5.1±3.2)‰; *n*=7, *p*<0.05, *t*-test).

3.3 *N_2 fixation rate (NFR)*

N_2 fixation activity was evident by the $^{15}N_2$ tracer assay, which caused bulk $\delta^{15}N_{PN}$ when terminating the incubation at no lesser than 35‰ for surface water samples. The surface N_2 fixation rate ranged between 0.6 and 2.6 nmol/(L·d) and averaged at (1.2±0.5) nmol/(L·d) (*n*=27, Fig. 2c). For the size fractionated N_2 fixation rate, <10 μm size fraction contributed predominantly (88%±6%, *n*=7; Fig. 4a) to the total rate between 135°E and 160°E. NFR seems to be higher at the subsurface (Fig. 3d). Depth-integrated N_2 fixation rate fell within a range between 150 and 480 μmol/(m^2·d) ((225±105) μmol/(m^2·d), *n*=9; Fig. 2d).

3.4 *Diazotroph community structure*

In 2013, UCYN-B comprised ~100% of the diazotroph community at the genus level based on the *nifH* gene abundance at most stations (9 of 11 stations visited). However, for the two stations at the western end of the sampling area, the relative abundance of *Trichodesmium* increased from ~8% at Sta. P2 to 96.8% at the westernmost Sta. P1 (Fig. 4b). A decreasing relative abundance of UCYN-B with increasing depth was observed at Sta. P11 (Fig. 4c).

3.5 *PP*

Surface water ^{14}C uptake derived PP averaged at (0.20±0.14) μmol/(L·d) over the study area, with the highest value (0.57 μmol/(L·d) being encountered at the westernmost station in the Luzon Strait (Fig. 2d). Depth-integrated PP averaged at (33.0±16.9) mmol/(m^2·d) (*n*=3).

4 Discussion

4.1 *Zonal variability of the diazotroph community structure in the WTNP*

This is the first time that a large-scale zonal distribution of the diazotroph community structure has been reported in the WTNP to the best of our knowledge. We found a clear longitudinal shift in 2013 in the diazotroph community structure from UCYN-B, which dominate over most of the WTNP, to the other well-known keystone diazotrophic cyanobacteria, *Trichodesmium* spp., that dominate in the vicinity of the western boundary current (Kuroshio) observed in this study (Fig. 4b). Consistently, a previous study in the adjacent western Pacific warm pool (13.5°N, 136°E) found high abundance of unicellular diazotrophic cyanobacteria *Crocosphaera watsonii* (Kim et al., 2017). UCYN-B are restricted to warm tropical waters and high abundance occurred in upper

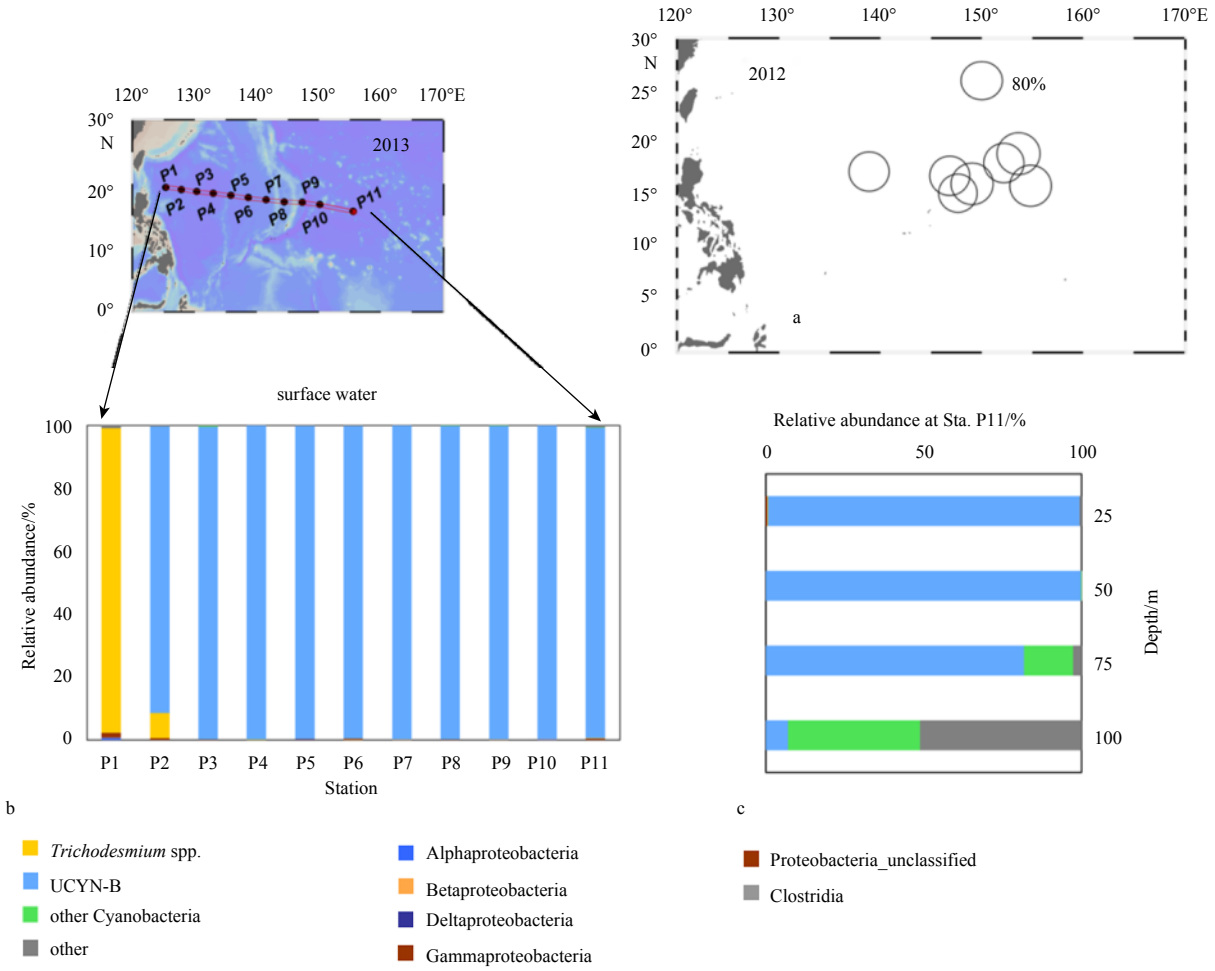

Fig. 4. Contribution of <10 μm size class to total N_2 fixation rate in surface waters (the circle area is proportional to their values) (a); meridional distribution of the diazotroph community structure at genus level based on *nifH* relative abundance in surface waters (note that the first layer sampled at the easternmost Sta. P11 is 25 m) (b); and depth profile (25–100 m) of the diazotroph community structure based on *nifH* relative abundance at Sta. P11 (c).

water column (as shown at station P11) which positively correlated to the temperature in the open ocean (Church et al., 2008; Shiozaki et al., 2014). Our finding is also consistent with previous observations of relatively abundant *Trichodesmium* in the Kuroshio Current, especially after its contact with the island mass along its main path (Zhang et al., 2012; Zhang et al., 2014; Shiozaki et al., 2014; Jiang et al., 2018). Our results along with available studies from other oceanic regions suggest that a spatial niche partitioning between diazotroph groups may be a common feature in the western tropical Pacific, with nano diazotrophs predominating the remote oceanic waters and micro *Trichodesmium* spp. usually predominating the waters close to large land mass, as in the western tropical South Pacific (WTSP) (Bonnet et al., 2009; Shiozaki et al., 2014). The diazotroph community structure is a key variable when looking into the dynamics of N_2 fixation and evaluating its biogeochemical importance in the context of the ongoing rapid climatic changes, thus needs to be further investigated in future studies in the WTNP (Church et al., 2009; Fu et al., 2014).

We propose that the zonal pattern of the diazotroph community structure and size fractionation of NFR may be tightly related to shift in environmental conditions in the WTNP. For instance, as a key limiting element for N_2 fixation, iron (Fe) variability is largely regulated both by the surface current (NEC) and atmospheric deposition (Jickells and Moore, 2015). In the study area, the prevailing westward-flowing NEC transports the most oligotrophic surface waters to the west, while it becomes more productive after receiving more nutrients (from aeolian input) westward. This is evidenced by a gradual eastward decrease in surface chlorophyll *a* (Figs 1 and 2a) and shoaling of SCM depth (Fig. 3e) along the NEC flow pathway. Although no concurrent dissolved iron (dFe) measurements in this study are available and published dFe data in surface waters of the WTNP are also lacking as well, study in the subtropical western North Pacific showed dFe generally <0.2 nmol/L in the surface waters (Brown et al., 2005), indicating a severe Fe deficiency in the remote WTNP waters as well. There is evidence suggesting a better adaptation for UCYN-B to poor Fe environments (especially for the more remote waters) than filamentous *Trichodesmium* (Saito et al., 2011; Jacq et al., 2014). Consistently, relatively active N_2 fixation can take place even over the sampled WTNP (Figs 3d and 4b). In contrast, the phosphorus scarcity, which is usually observed in the warm open oceanic waters, may be alleviated by diazotrophs via dissolved organic phosphorus (DOP) utilization (Dyhrman and Haley, 2006; Dyhrman et al., 2006). Consistently, macro-scale exhaustion of surface phosphate along with relat-

ively active N_2 fixation has been observed in the western Pacific Ocean (Hashihama et al., 2009), probably indicating the complementary source of P (such as utilization of DOP) by N_2 fixers. In any case, the exact causes for the shift in diazotroph community structure and controls on N_2 fixation characteristics need to be investigated intensively in the WTNP.

4.2 *N_2 fixation as a new N source to the WTNP ecosystem*

N_2 fixation rates in the present study generally fall in the range reported in the adjacent Western Pacific Warm Pool (Shiozaki et al., 2017) and Sta. ALOHA in the NPSG (Böttjer et al., 2017). Depth-integrated N_2 fixation rate in 2012 ((271.7±180.4) μmol/(m²·d), *n*=3) are generally higher than the reported total atmospheric N deposition flux of 26 μmol/(m²·d) in the western Pacific Ocean (Martino et al., 2014). Our concurrent measurements in 2012 show that depth-integrated N_2 fixation accounts for 6.2%±3.7% of the depth-integrated PP ((33.0±16.9) mmol/(m²·d), *n*=3) after Redfield stoichiometry (C:N=106:16), which is similar to the surface ratio (5.9%±3.9%). If we adopt the typical *f*-ratio (=nitrate assimilation/PP) value range (0.05–0.20) reported in the adjacent Western Pacific Warm Pool with a similar LNLC condition (Shiozaki et al., 2013), we estimate that N_2 fixation may represent a new N flux comparable (30% or higher) to that of nitrate assimilation. The oligotrophic oceanic system, such as the Western Pacific Warm Pool, is generally featured by rapid recycling (low *f*-ratios) along with active N_2 fixation (Shiozaki et al., 2013), thereby suggesting that the contribution of N_2 fixation in local C and N cycles probably exceeds such NFR/PP ratios in the WTNP.

The influence of N_2 fixation to local biogeochemistry is reflected also by the relatively low $\delta^{15}N_{PN}$ values (1.9‰±1.3‰ for surface PN), especially for the western part of the study area (Fig. 2b). Although both N_2 fixation and atmospheric deposition can input isotopically light N to the surface ocean (Zhang et al., 2011; Ren et al., 2017), the latter is less likely a dominant factor controlling $\delta^{15}N_{PN}$ distribution in this study. As our results show that the stations closer to the major land mass, which are expected to receive more aeolian N, are actually featured by much higher (rather than lower) $\delta^{15}N_{PN}$ values (Fig. 2b). Hence, we suggest that N_2 fixation is the main factor for the observed spatial variation of $\delta^{15}N_{PN}$ values. Consistently, low $\delta^{15}N$ values were also observed in the suspended particulate organic matter during 2014 (Yang et al., 2017) and sediment trap samples in the WTNP (Kim et al., 2017), and N_2 fixation has been speculated to be the main reason. N_2 fixation derived fresh organic matter is featured by relatively ^{15}N-depleted isotope ratios, ~1‰, because the substrate for this pathway (atmospheric N_2 $\delta^{15}N$=0‰) is depleted in ^{15}N and an insignificant amount of isotope fractionation takes place during this process (Carpenter et al., 1997).

The WTNP is a region vulnerable to climate variability and the main forcing mechanisms include warming, freshening, and changed atmospheric dust deposition (Cravatte et al., 2009; Kodama et al., 2011; Jickells and Moore, 2015). Therefore, how N_2 fixation and relevant biological pump processes in the WTNP may respond to climatic changes needs to be addressed in future studies (Kim et al., 2017).

5 Conclusions

Our results showed that unicellular fraction is the dominant contributor to N_2 fixation during sampling periods in summers of 2012 and 2013 in most of the sampling area, whereas microdiazotroph *Trichodesmium* dominate in the west end (Kuroshio). Such zonal variations of diazotroph community structure may be a complex result of shift in environmental conditions in the subregions of the WTNP, i.e., NEC transporting most oligotrophic waters westward while atmospheric dust deposition increase on the other hand. N_2 fixation acts as a significant exogenous new N source and plays an important in driving biogeochemical cycles in the WTNP, wherein enhanced environmental changes occur in the context of climatic changes.

Acknowledgements

We are grateful to China Ocean Mineral Resources R&D Association (COMRA) for arranging the cruise and providing background data. We thank the captain and crew of the R/V *Haiyang Liuhao* for their invaluable assistance while sampling on the sea. We thank Xiguang Deng, Binbin Guo, Youcheng Bai, Xinyu Xu for technical assistance. Thanks are also due to COMRA scientists, Jianfang Chen, Zhi Yang and Wei Zhuang, for helpful discussions. We also thank the invaluable comment by anonymous reviewers.

References

Bonnet S, Biegala I C, Dutrieux P, et al. 2009. Nitrogen fixation in the western equatorial Pacific: Rates, diazotrophic cyanobacterial size class distribution, and biogeochemical significance. Global Biogeochemical Cycles, 23(3): GB3012

Böttjer D, Dore J E, Karl D M, et al. 2017. Temporal variability of nitrogen fixation and particulate nitrogen export at Station ALOHA. Limnology and Oceanography, 62(1): 200–216, doi: 10.1002/lno.10386

Brown M T, Landing W M, Measures C I. 2005. Dissolved and particulate Fe in the western and central North Pacific: Results from the 2002 IOC cruise. Geochemistry, Geophysics, Geosystems, 6(10): Q10001, doi: 10.1029/2004GC000893

Cabrera O, Villanoy C, Alabia I D, et al. 2015. Shifts in chlorophyll a off Eastern Luzon, Philippines, associated with the North Equatorial Current bifurcation latitude. Oceanography (Washington D.C.), 28(4): 46–53, doi: 10.5670/oceanog.2015.80

Capone D G, Zehr J P, Paerl H W, et al. 1997. *Trichodesmium*, a globally significant marine cyanobacterium. Science, 276(5316): 1221–1229, doi: 10.1126/science.276.5316.1221

Caporaso J G, Kuczynski J, Stombaugh J, et al. 2010. QIIME allows analysis of high-throughput community sequencing data. Nature Methods, 7(5): 335–336, doi: 10.1038/nmeth.f.303

Carpenter K E. 1998. An introduction to the oceanography, geology, biogeography, and fisheries of the tropical and subtropical western and central Pacific. In: Carpenter K E, Niem V H, eds. FAO Species Identification Guide for Fishery Purposes. Rome: The Living Marine Resources of the Western Central Pacific

Carpenter E J, Harvey H R, Fry B, et al. 1997. Biogeochemical tracers of the marine cyanobacterium *Trichodesmium*. Deep Sea Research Part I: Oceanographic Research Papers, 44(1): 27–38, doi: 10.1016/S0967-0637(96)00091-X

Carpenter E J, Montoya J P, Burns J, et al. 1999. Extensive bloom of a N_2-fixing diatom/cyanobacterial association in the tropical Atlantic Ocean. Marine Ecology Progress Series, 185: 273–283, doi: 10.3354/meps185273

Chen Y L L, Chen H Y, Lin Y H, et al. 2014. The relative contributions of unicellular and filamentous diazotrophs to N_2 fixation in the South China Sea and the upstream Kuroshio. Deep Sea Research Part I: Oceanographic Research Papers, 85: 56–71, doi: 10.1016/j.dsr.2013.11.006

Church M J, Björkman K M, Karl D M, et al. 2008. Regional distributions of nitrogen-fixing bacteria in the Pacific Ocean. Limnology and Oceanography, 53(1): 63–77, doi: 10.4319/lo.2008.53.1.0063

Church M J, Mahaffey C, Letelier R M, et al. 2009. Physical forcing of nitrogen fixation and diazotroph community structure in the North Pacific subtropical gyre. Global Biogeochemical Cycles, 23(2): GB2020

Clement A, DiNezio P. 2014. The tropical Pacific Ocean-back in the driver's seat? Science, 343(6174): 976–978, doi: 10.1126/science.

1248115
Cravatte S, Delcroix T, Zhang Dongxiao, et al. 2009. Observed freshening and warming of the western Pacific Warm Pool. Climate Dynamics, 33(4): 565–589, doi: 10.1007/s00382-009-0526-7
Deutsch C, Sarmiento J L, Sigman D M, et al. 2007. Spatial coupling of nitrogen inputs and losses in the ocean. Nature, 445(7124): 163–167, doi: 10.1038/nature05392
Dyhrman S T, Chappell P D, Haley S T, et al. 2006. Phosphonate utilization by the globally important marine diazotroph *Trichodesmium*. Nature, 439(7072): 68–71, doi: 10.1038/nature04203
Dyhrman S T, Haley S T. 2006. Phosphorus scavenging in the unicellular marine diazotroph *Crocosphaera watsonii*. Applied and Environmental Microbiology, 72(2): 1452–1458, doi: 10.1128/AEM.72.2.1452-1458.2006
Fish J A, Chai Benli, Wang Qiong, et al. 2013. FunGene: the functional gene pipeline and repository. Fronters in Microbiology, 4: 291, doi: 10.3389/fmicb.2013.00291
Fu F X, Yu E, Garcia N S, et al. 2014. Differing responses of marine N_2 fixers to warming and consequences for future diazotroph community structure. Aquatic Microbial Ecology, 72(1): 33–46, doi: 10.3354/ame01683
Gruber N, Sarmiento J L. 1997. Global patterns of marine nitrogen fixation and denitrification. Global Biogeochemical Cycles, 11(2): 235–266, doi: 10.1029/97GB00077
Hansen H P, Koroleff F. 1999. Determination of nutrients. In: Grasshoff K, Kremling K, Ehrhardt M, eds. Methods of Seawater Analysis. 3rd ed. Weinheim: Wiley-VCH, 170–198
Hashihama F, Furuya K, Kitajima S, et al. 2009. Macro-scale exhaustion of surface phosphate by dinitrogen fixation in the western North Pacific. Geophysical Research Letters, 36(3): L03610
Jacq V, Ridame C, L'Helguen S, et al. 2014. Response of the unicellular diazotrophic cyanobacterium *Crocosphaera watsonii* to iron limitation. PLoS One, 9(1): e86749, doi: 10.1371/journal.pone.0086749
Jiang Z B, Li H L, Zhai H C, et al. 2018. Seasonal and spatial changes in *Trichodesmium* associated with physicochemical properties in East China Sea and southern Yellow Sea. Journal of Geophysical Research: Biogeosciences, 123(2): 509–530, doi: 10.1002/2017JG004275
Jickells T, Moore C M. 2015. The importance of atmospheric deposition for ocean productivity. Annual Review of Ecology, Evolution, and Systematics, 46: 481–501, doi: 10.1146/annurev-ecolsys-112414-054118
Karl D M, Michaels A F, Bergman B, et al. 2002. Dinitrogen fixation in the world's oceans. Biogeochemistry, 57(1): 47–98, doi: 10.1023/A:1015798105851
Kim D, Jeong J H, Kim T W, et al. 2017. The reduction in the biomass of cyanobacterial N_2 fixer and the biological pump in the Northwestern Pacific Ocean. Scientific Reports, 7: 41810, doi: 10.1038/srep41810
Kitajima S, Furuya K, Hashihama F, et al. 2009. Latitudinal distribution of diazotrophs and their nitrogen fixation in the tropical and subtropical western North Pacific. Limnology and Oceanography, 54(2): 537–547, doi: 10.4319/lo.2009.54.2.0537
Klawonn I, Lavik G, Böning P, et al. 2015. Simple approach for the preparation of $^{15-15}N_2$-enriched water for nitrogen fixation assessments: evaluation, application and recommendations. Frontiers in Microbiology, 6: 769
Kodama T, Furuya K, Hashihama F, et al. 2011. Occurrence of rain-origin nitrate patches at the nutrient-depleted surface in the East China Sea and the Philippine Sea during summer. Journal of Geophysical Research: Oceans, 116(C8): C08003
Lehodey P, Bertignac M, Hampton J, et al. 1997. El Nino Southern Oscillation and tuna in the Western Pacific. Nature, 389(6652): 715–718, doi: 10.1038/39575
Martino M, Hamilton D, Baker A R, et al. 2014. Western Pacific atmospheric nutrient deposition fluxes, their impact on surface ocean productivity. Global Biogeochemical Cycles, 28(7): 712–728, doi: 10.1002/2013GB004794
Mohr W, Großkopf T, Wallace D W R, et al. 2010. Methodological underestimation of oceanic nitrogen fixation rates. PLoS One, 5(9): e12583, doi: 10.1371/journal.pone.0012583
Montoya J P, Voss M, Kähler P, et al. 1996. A simple, high-precision, high-sensitivity tracer assay for N2 fixation. Applied and Environmental Microbiology, 62(3): 986–993
Montoya J P, Holl C M, Zehr J P, et al. 2004. High rates of N_2 fixation by unicellular diazotrophs in the oligotrophic Pacific Ocean. Nature, 430(7003): 1027–1031, doi: 10.1038/nature02824
Qiu Bo, Rudnick D L, Cerovecki I, et al. 2015. The pacific north equatorial current: new insights from the origins of the Kuroshio and Mindanao Currents (OKMC) Project. Oceanography, 28(4): 24–33, doi: 10.5670/oceanog.2015.78
Ren Haojia, Chen Yichi, Wang X T, et al. 2017. 21st-century rise in anthropogenic nitrogen deposition on a remote coral reef. Science, 356(6339): 749–752, doi: 10.1126/science.aal3869
Saito M A, Bertrand E M, Dutkiewicz S, et al. 2011. Iron conservation by reduction of metalloenzyme inventories in the marine diazotroph *Crocosphaera watsonii*. Proceedings of the National Academy of Sciences of the United States of America, 108(6): 2184–2189, doi: 10.1073/pnas.1006943108
Shiozaki T, Kodama T, Furuya K. 2014. Large-scale impact of the island mass effect through nitrogen fixation in the western South Pacific Ocean. Geophysical Research Letters, 41(8): 2907–2913, doi: 10.1002/2014GL059835
Shiozaki T, Kodama T, Kitajima S, et al. 2013. Advective transport of diazotrophs and importance of their nitrogen fixation on new and primary production in the western Pacific warm pool. Limnology and Oceanography, 58(1): 49–60, doi: 10.4319/lo.2013.58.1.0049
Shiozaki T, Bombar D, Riemann L, et al. 2017. Basin scale variability of active diazotrophs and nitrogen fixation in the North Pacific, from the tropics to the subarctic Bering Sea. Global Biogeochemical Cycles, 31(6): 996–1009, doi: 10.1002/2017GB005681
Wang Q, Garrity G M, Tiedje J M, et al. 2007. Naive Bayesian classifier for rapid assignment of rRNA sequences into the new bacterial taxonomy. Applied and Environmental Microbiology, 73(16): 5261–5267, doi: 10.1128/AEM.00062-07
Wannicke N, Benavides M, Dalsgaard T, et al. 2018. New perspectives on nitrogen fixation measurements using $^{15}N_2$ gas. Frontiers in Marine Science, 5: 120, doi: 10.3389/fmars.2018.00120
Wolfe D A, Schelske C L. 1967. Liquid scintillation and Geiger counting efficiencies for Carbon-14 incorporated by marine phytoplankton in productivity measurements. ICES Journal of Marine Science, 31(1): 31–37, doi: 10.1093/icesjms/31.1.31
Yang Guang, Li Chaolun, Guilini K, et al. 2017. Regional patterns of $\delta^{13}C$ and $\delta^{15}N$ stable isotopes of size-fractionated zooplankton in the western tropical North Pacific Ocean. Deep Sea Research Part I: Oceanographic Research Papers, 120: 39–47, doi: 10.1016/j.dsr.2016.12.007
Zehr J P, Turner P J. 2001. Nitrogen fixation: Nitrogenase genes and gene expression. Methods in Microbiology, 30: 271–286, doi: 10.1016/S0580-9517(01)30049-1
Zehr J P, Waterbury J B, Turner P J, et al. 2001. Unicellular cyanobacteria fix N_2 in the subtropical North Pacific Ocean. Nature, 412(6847): 635–638, doi: 10.1038/35088063
Zhang Run, Chen Min, Cao Jianping, et al. 2012. Nitrogen fixation in the East China Sea and southern Yellow Sea during summer 2006. Marine Ecology Progress Series, 447: 77–86, doi: 10.3354/meps09509
Zhang Run, Chen Min, Ma Qiang, et al. 2011. Latitudinal distribution of nitrogen isotopic composition in suspended particulate organic matter in tropical/subtropical seas. Isotopes in Environmental and Health Studies, 47(4): 489–497, doi: 10.1080/10256016.2011.622442
Zhang Dongsheng, Lu Douding, Li Hongliang, et al. 2014. Seasonal dynamics of *Trichodesmium* in the northern East China Sea. Continental Shelf Research, 88: 161–170, doi: 10.1016/j.csr.2014.05.016

Supplementary information:

Table S1. Statistics information of *nifH* sequences from 14 samples.

Table S2. Custom primers including *nifH1* and *nifH2*, adaptor and sample specific tags used (underlined) for the second-round PCR reactions and pyrosequencing.

Fig. S1. Comparison of natural δ^{15}N values in each PON pool: measured bulk, mass balance calculated bulk, <10 μm and >10 μm fraction, respectively.

The supplementary information is available online at https://doi.org/10.1007/s13131-019-1513-4 and www.hyxb.org.cn/aosen/ch/index.aspx. The supplementary information is published as submitted, without typesetting or editing. The responsibility for scientific accuracy and content remains entirely with the authors.